Nuclear Materials and Energy 16 (2018) 263–266

Contents lists available at ScienceDirect

Nuclear Materials and Energy

journal homepage: www.elsevier.com/locate/nme

Effect of heat load on microstructural development in an irradiated low alloy steel

Shunta Goto[a,*], N. Hashimoto[b]

[a] Graduate School of Engineering, Hokkaido University, N13 W8, Kita-ku, Sapporo 060-8628, Japan
[b] Faculty of Engineering, Hokkaido University, N13 W8, Kita-ku, Sapporo 060-8628, Japan

ARTICLE INFO

Keywords:
Low alloy steel
Electron irradiation
Annealing
Irradiation damage

ABSTRACT

To investigate the influence of heat load on microstructure change, we conducted in-situ experiments of annealing and irradiation for a model alloy (Fe-0.75Mn-0.47Mo-0.45Ni) using a multi-beam high voltage electron microscope. Electron-irradiation resulted in the formation of black dots in the model alloy. It is noted that some of black dots grew and changed to dislocation loops, but some did not. Furthermore, the 500 °C annealing to the electron-irradiated sample resulted in the shrinkage and/or the disappearance of black dots and small loops (<10 nm). It is suggested that the annealing would cause the release of interstitial atoms from small loops, which could flow into adjacent larger loops or diffuse to the surface.

1. Introduction

Mechanical property change in reactor pressure vessel steels induced by neutron irradiation is a key issue for safe and longer operation of reactors. The embrittlement is attributed to nano-scale microstructural features such as copper rich precipitates, matrix damage and grain boundary segregation [1–9]. While precipitation and segregation have been extensively studied [10], it is still unclear, what the nature and the main mechanisms of the formation of matrix damage are. In addition, if a severe accident was to happen and the coolant system stopped, the temperature of reactor components could quickly exceed the normal operation temperature. Systematic and specific research on the change of microstructure after a potential severe accident is necessary and should include the effect of heat load on irradiated materials. To investigate the influence of heat load on microstructure change, we conducted in-situ experiments of irradiation and annealing to a model alloy (Fe-0.75Mn-0.47Mo-0.45Ni) by a multi-beam high voltage electron microscope (HVEM). Electron irradiation (in-situ observation) experiment would be powerful tool for the direct investigation of secondary defect behavior under irradiation, which in impossible under neutron irradiation. The important parameters of microstructure change are the change in size and number density of loops and black dots during electron irradiation and annealing.

2. Experimental

The materials used for this study was a model alloy based on a low alloy steel used for reactor pressure vessels in Light Water Reactors. Table 1 indicates the chemical composition of the model alloy. The low alloy steel was arc melted, and then rolled down to 0.2 mm in thick. Sheets of the steel were mechanically ground down to 0.10 mm in thick. Discs of 3 mm in diameter were punched out and solution-annealed at 800 °C for 2 h in vacuum, followed by electro-polishing for the irradiation and tempering experiment. The conditions for the electro-polishing are shown in Table 2. The in-situ electron irradiation experiment was carried out using a high voltage electron microscope (HVEM JEM-ARM-1300) operating at 1250 kV at Hokkaido University. In-situ electron irradiation (the 1st irradiation) was carried out at the damage rate of 3.0×10^{-4} dpa/s to 0.2 dpa at 290 °C. After the 1st irradiation experiment, additional irradiation (the 2nd irradiation) and annealing experiment were performed in the HVEM. The 2nd irradiation to the 1st-irradiated sample was carried out at 500 °C to 0.14 dpa (total dose was 0.34 dpa). The annealing experiment at 500 °C for 90 min was performed to the 1st irradiated sample. The irradiation conditions and annealing condition are summarized in Table 3. The temperature of annealing experiment was decided based on the increase in average temperature of reactor pressure vessel after a severe accident. The temperature history of the irradiation and tempering experiment is shown in Fig. 1. To ensure reliability, more than 100 of loops were analyzed. In the calculation of number density, the thickness of the irradiated area was estimated by thickness fringe. Using an appropriate reflection g, we can calculate the extinction distance: ζ_g. For example, in the case of $g = 011$, the $\zeta_{g=011}$ of α-Fe is about 29 nm. In the two-beam condition, the n_{th} bright fringe from the edge of the wedge shape

* Corresponding author.
E-mail address: hasimoto@eng.hokudai.ac.jp (S. Goto).

https://doi.org/10.1016/j.nme.2018.06.020
Received 6 December 2017; Received in revised form 28 June 2018; Accepted 28 June 2018
Available online 06 July 2018

Table 1
Chemical comosition of low alloy model steel (wt.%).

Fe	Mn	Mo	Ni	C	Si	P	Cu	S
Bal.	0.75	0.47	0.45	0.001	<0.01	<0.003	<0.003	0.0003

Table 2
Electro-polishing condition.

Electrolyte	Acetate:Perchloric acid = 19:1
Voltage (V)	80.0 ~ 90.0
Current (mA)	90 ~ 120
Temperature (°C)	14.0 ~ 17.0

Table 3
Condition of electron irradiation and annealing.

Acceleration voltage	1250 keV
1st electron irradiation	290 °C, 3.0×10^{-4} dpa/s, 0.2 dpa
2nd electron irradiation	500 °C, 2.6×10^{-5} dpa/s, 0.14 dpa after the 1st electron irradiation
Annealing	500 °C, 90 min. after the 1st electron irradiation

Table 4
Number density and size of dislocation loops and black dots during the 1st irradiation.

Dose	0.10 dpa	0.15 dpa	0.20 dpa
Number density/m^{-3}	5.8×10^{21}	5.5×10^{21}	3.3×10^{21}
Size/nm	8.90	11.6	17.0

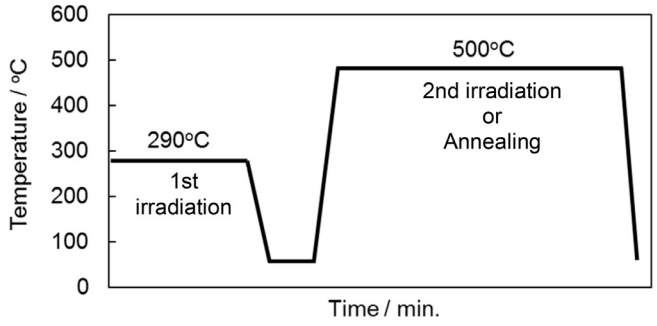

Fig. 1. History of irradiaion and aging experiment for low alloy steel.

sample can give the thickness value of 29*n* nm. The thickness of the 10_{th} fringe area can be estimated to be 290 nm. This would be the best way to estimate the thickness of wedge shape samples.

3. Results

3.1. Microstructural development during the 1st irradiation at 290 °C

Typical microstructural development during the 1st irradiation experiment using HVEM is shown in Fig. 2. Both bright field and weak beam dark field images were taken in the condition of $\boldsymbol{B} \sim [111]$, $\boldsymbol{g} = 110$, and $s > 0$. Irradiation-induced black dots were observed in the early stage of irradiation at 290 °C. Some black dots grew and changed to dislocation loops as increasing in dose, while the other did not. On the other hand, no voids were observed in matrix. The total number density and the average diameter of loops and black dots were 3.3×10^{21} m^{-3} and 16.9 nm, respectively.

3.2. Microstructural development during annealing at 500 °C

After the 1st electron irradiation at 290 °C to 0.2 dpa, annealing was carried out at 500 °C for 90 min. Fig. 3 shows the microstructural changes before and after annealing. The imaging condition was $\boldsymbol{B} \sim [111]$, $\boldsymbol{g} = 110$, and $s > 0$. The annealing experiment to the 1st irradiated sample exhibited the shrinkage or disappearance of black dots and small loops (< 10 nm). The number density and the size of dislocation loops and black dots are summarized in Table 5. The annealing experiment resulted in a decrease in the number density and an increase in the size of black dots and loops.

3.3. Microstructural development during the 2nd irradiation at 500 °C

The microstructural change after the 2nd irradiation is shown in Fig. 4. The imaging condition was $\boldsymbol{B} \sim [111]$, $\boldsymbol{g} = 110$, and $s > 0$. During the 2nd irradiation, some dislocation loops grew by interacting with the other loops. As listed in Table 5, the 2nd irradiation resulted in the remarkable decrease in the number density and the increase in the size of black dots and loops compared to annealed sample. The size distribution of black dots and loops before and after the 2nd irradiation was shown in Fig. 6. The size distribution of loops in the 1st and 2nd irradiated sample changed more significantly than that of annealed after the 1st irradiated sample.

4. Discussion

During the 1st irradiation, some black dots grew and changed to loops as increasing in dose, while the others did not. From this result, it

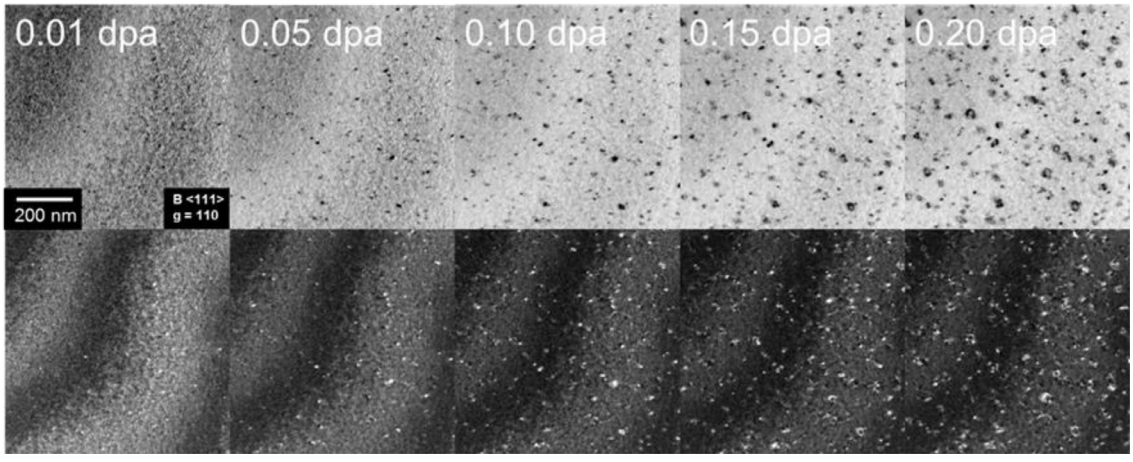

Fig. 2. Microstructural development in the low alloy steel during 1st electron irradiation at 290 °C to 0.2 dpa.

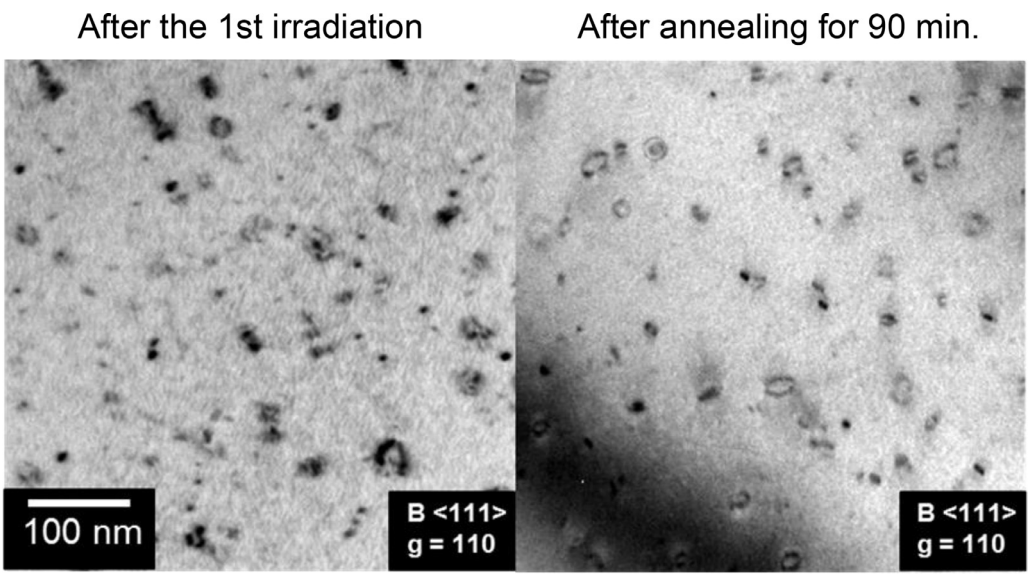

Fig. 3. Microstructural change the irradiated low alloy steel before and after annealing at 500 °C.

Table 5
Number density and size of black dots and loops after the 1st irradiation, annealing after the 1st irradiation, and the 2nd irradiation.

	1st irradiation	Annealing after 1st irradiation	2nd irradiation
Number density/m^{-3}	2.49×10^{21}	9.83×10^{20}	3.88×10^{20}
Mean diameter/nm	16.4	18.6	92.2

appears that there are two types of irradiation-induced loops with different growth rates. The previous observations of irradiated iron have indicated that the irradiation-induced loops have $\boldsymbol{b} = a < 100 >$ [11,12]. While, the $a/2 < 111 >$ loops would be favorable in terms of energy [13]. A molecular dynamics simulation proposed an alternative mechanism for the nucleation and growth of TEM visible $a < 100 >$ loop [14]. The $a < 100 >$ loops are postulated to form as a result of direct interactions of mobile $a/2 < 111 >$ clusters of comparable size. The $a < 100 >$ loops are stable and practically immobile, allowing for the absorption of other small $a/2 < 111 >$ clusters thereby allowing $a < 100 >$ loop growth up to TEM observation sizes. In this study, the visible loops formed during irradiation would be $a < 100 >$ or $a/2 < 111 >$ loops, however, the

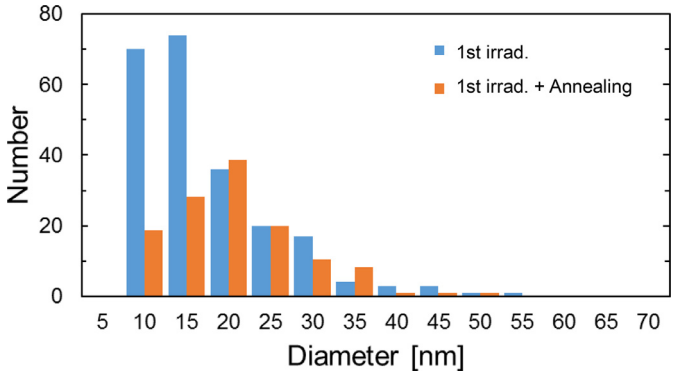

Fig. 5. Comparison of the size distribution of loops between after the 1st irradiation and after the annealing.

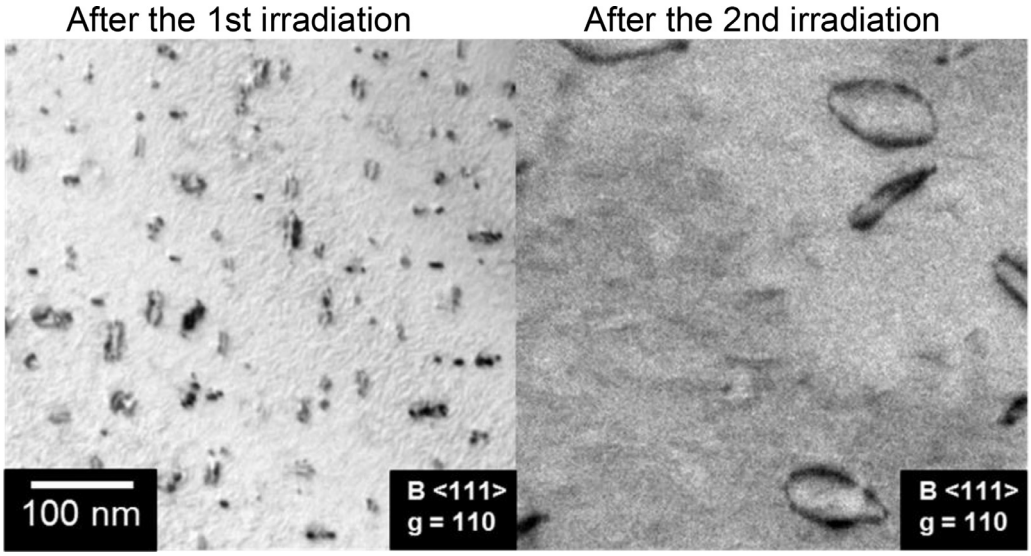

Fig. 4. Microstructural change in the irradiated low alloy steel before and after the 2nd irradiation at 500 °C.

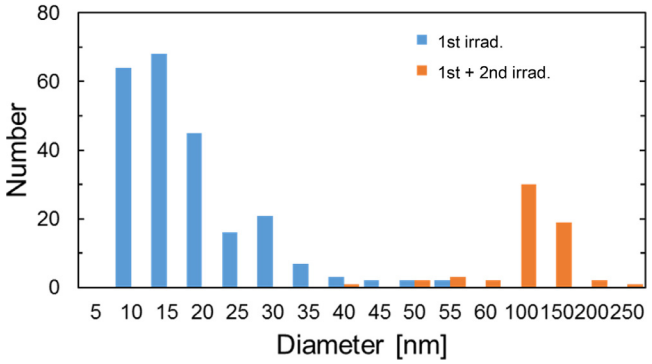

Fig. 6. Comparison of the size distribution of loops between after the 1st irradiation and after the 2nd irradiation.

difference of growth rate between a < 100 > and a/2 < 111 > was unknown. The detail analysis would be needed. On the other hand, irradiation-introduced excess vacancies could also get together and form vacancy type clusters in matrix. In this study, no voids were observed in the model alloy after the 1st irradiation, however there is a possibility of the invisible voids or vacancy type loop formation. The annealing experiment would be one of appropriate approaches to understand this issue.

In this study, the annealing at 500 °C for the 1st irradiated sample exhibited the shrinkage or disappearance of small loops, which resulted in the decrease in the number density and the slight increase in the size of black dots and loops. With assuming loops to be interstitial type, the amount of interstitial flow to the other loops was estimated from the total circumferential lengths of dislocation loops. The total circumference before and after annealing was estimated to be 11.0 μm and 7.4 μm, respectively. Since the circumference length decreases after annealing, it suggests that the part of dislocation loops and black dots could be dissolved in matrix or diffused out during the annealing. The proportion of the dissolved loops and black dots was estimated to be about 45%. The diffusion distance of iron atoms was calculated using the formula:

$$d = (Dt)^{1/2}$$

with t, the annealing time and D the iron self-diffusion coefficient given by

$$D = D_o exp(-Q/RT)$$

where R is gas constant, T is the annealing temperature (773 K), and Q the migration energy (251 kJ/mol). From the above equation, the diffusion distance would be about 660 nm. The thickness of the irradiated area measured by thickness fringe was about 200–300 nm, suggesting that the remaining 54% of loops and black dots would diffuse to the surface and shrink and disappear with releasing interstitial atoms. Fig. 5 shows the size distribution of black dots and loops before and after aging at 500 °C. From these results, it is suggested that the annealing would cause the release of interstitial atoms from small loops and some interstitials flow into relatively larger loops. Previous study reported that the effect of post-irradiation annealing was the reduction of the total volume fraction of irradiation-induced clusters with increasing annealing temperature [15]. This observation immediately suggests that a certain number of irradiation-induced clusters essentially dissolve [15]. It is noted that the dissolution of the irradiation-induced clusters would indicate the release of not only interstitials but also vacancies. With assuming loops to be vacancy type, a certain amount of vacancies dissolved in matrix, leading to the reduction of small clusters.

The 2nd irradiation at 500 °C can produce additional interstitials and vacancies in the 1st irradiated area. In this case, the nucleation of interstitial loops may be reduced due to decreased concentration (increased mobility) of irradiation-produced interstitial atoms at higher temperatures, as compared to lower temperatures [16]. Introduced interstitials would preferentially flow into loops on the basis of the dislocation bias, which led to the increase in size of loops. Furthermore, larger loops had interaction with each other, resulting in the decrease in loop density. While, vacancies would be mobile at this temperature and easily diffuse away to specimen surface. This would be the reason of no voids found after the 2nd irradiation.

5. Summary

To investigate the influence of heat load on microstructure change, in-situ experiments of irradiation and annealing were carried out to the low alloy steel. The results are summarized as below.

(1) Irradiation-induced black dots were observed in the early stage of irradiation.
(2) Some black dots grew and changed to loops as increasing in dose, while the others did not. It seems that there are two types of irradiation-induced loops with different growth rates.
(3) The annealing experiment showed that tiny black dots and smaller loops tend to shrink or disappear during annealing, suggesting that the release of interstitial atoms from small loops occurs and those interstitials flow into relatively larger loops or diffuse to surface.

Acknowledgment

The authors wish to thank Mr. Wang for operating TEM and to Mr. Ohkubo and Mr. Tanioka for operating the High Voltage Electron Microscope at Hokkaido University.

Supplementary materials

Supplementary material associated with this article can be found, in the online version, at doi:10.1016/j.nme.2018.06.020.

References

[1] D. Terentyev, X. He, G. Bonny, A. Bakaev, E. Zhurkin, L. Malerba, J. Nucl. Mater. 457 (2015) 173–181.
[2] P.D. Styman, J.M. Hyde, K. Wilford, A. Morley, G.D.W. Smith, Prog. Nucl. Energy. 57 (2012) 86–92.
[3] G.R. Odette, G.E. Lucas, Radiat. Eff. Defects Solids. 144 (1998) 189–231.
[4] K. Fukuya, K. Ohno, H. Nakata, S. Dumbill, J.M. Hyde, J. Nucl. Mater. 312 (2003) 163–173.
[5] K. Fujii, K. Fukuya, J. Nucl. Mater. 336 (2005) 323–330.
[6] C. English, J. Hyde, Elsevier, 2012, pp. 151–180.
[7] R.G. Carter, N. Soneda, K. Dohi, J.M. Hyde, C.A. English, W.L. Server, J. Nucl. Mater. 298 (2001) 211–224.
[8] M. Bachhav, G. Robert Odette, E.A. Marquis, J. Nucl. Mater. 454 (2014) 381–386.
[9] Z. Zhai, Y. Miyahara, H. Abe, Y. Watanabe, J. Nucl. Mater. 452 (2014) 133–140.
[10] W.J. Phythian, C.A. English, J. Nucl. Mater. 205 (1993) 162–177.
[11] I.M. Robertson, M.L. Jenkins, C.A. English, J. Nucl. Mater. 108/109 (1982) 209–221.
[12] M.A. Kirk, M.L. Jenkins, H. Fukushima, J. Nucl Mater. 276 (2000) 50–58.
[13] J.M. Harder, D.J. Bacon, Phil. Mag. A 58 (1988) 165–178.
[14] J. Marian, B.D. Wirth, Phys. Rev. Let. 88 (2002) 255507.
[15] F. Bergner, A. Ulbricht, P. Lindner, U. Keiderling, L. Malerba, J. Nucl. Mater. 454 (2014) 22–27.
[16] N. Hashimoto, S. Goto, S. Inoue, E. Suzuki, J. Nucl. Mater. 495 (2017) 1–5.